

SCIENTIFIC REPORTS



OPEN

Identification of a novel inactivating mutation in Isocitrate Dehydrogenase 1 (IDH1-R314C) in a high grade astrocytoma

Received: 17 February 2016

Accepted: 06 July 2016

Published: 27 July 2016

Sanne A. M. van Lith¹, Anna C. Navis¹, Krissie Lenting¹, Kiek Verrijp¹, Jan T. G. Schepens², Wiljan J. A. J. Hendriks², Nil A. Schubert¹, Hanka Venselaar³, Ron A. Wevers⁴, Arno van Rooij⁴, Pieter Wesseling^{1,5}, Remco J. Molenaar⁶, Cornelis J. F. van Noorden⁶, Stefan Pusch⁷, Bastiaan Tops¹ & William P. J. Leenders¹

The majority of low-grade and secondary high-grade gliomas carry heterozygous hotspot mutations in cytosolic isocitrate dehydrogenase 1 (*IDH1*) or the mitochondrial variant *IDH2*. These mutations mostly involve Arg132 in *IDH1*, and Arg172 or Arg140 in *IDH2*. Whereas IDHs convert isocitrate to alpha-ketoglutarate (α -KG) with simultaneous reduction of NADP⁺ to NADPH, these IDH mutants reduce α -KG to D-2-hydroxyglutarate (D-2-HG) while oxidizing NADPH. D-2-HG is a proposed oncometabolite, acting via competitive inhibition of α -KG-dependent enzymes that are involved in metabolism and epigenetic regulation. However, much less is known about the implications of the metabolic stress, imposed by decreased α -KG and NADPH production, for tumor biology. We here present a novel heterozygous *IDH1* mutation, *IDH1*^{R314C}, which was identified by targeted next generation sequencing of a high grade glioma from which a mouse xenograft model and a cell line were generated. *IDH1*^{R314C} lacks isocitrate-to- α -KG conversion activity due to reduced affinity for NADP⁺, and differs from the *IDH1*^{R132} mutants in that it does not produce D-2-HG. Because *IDH1*^{R314C} is defective in producing α -KG and NADPH, without concomitant production of the D-2-HG, it represents a valuable tool to study the effects of *IDH1*-dysfunction on cellular metabolism in the absence of this oncometabolite.

Diffuse gliomas are primary tumors of the brain that are thought to develop from (precursors of) astrocytes or oligodendrocytes. Based on histopathology and according to WHO guidelines, these cancers are classified as grade II-IV astrocytomas or grade II-III oligodendrogliomas^{1,2}. The disease is essentially incurable and median overall survival of patients with grade IV astrocytoma (glioblastoma, the most malignant variant) is only 15 months, despite chemo- and radiotherapy³.

In 2008, somatic mutations in the isocitrate dehydrogenase genes *IDH1* and *IDH2* were identified in the large majority of low grade gliomas and secondary glioblastomas⁴. These mutations are always heterozygous and mostly involve the same amino acid residues; Arg132 in the cytosolic *IDH1* and Arg172 or Arg140 in the mitochondrial *IDH2*⁵⁻⁷. In glioma, the majority of *IDH* mutations are found in *IDH1*, and about 90% are *IDH1*^{R132H}. Extensive research has revealed that these mutations are neomorphic gain-of-function mutations, resulting in the conversion of α -ketoglutarate (α -KG), the normal product of *IDH*-mediated decarboxylation of isocitrate, to D-2-hydroxyglutarate (D-2-HG) which can accumulate to millimolar concentrations⁸. During the conversion of α -KG to D-2-HG by the mutant enzyme, NADPH is oxidized.

¹Department of Pathology, Radboudumc, Nijmegen, The Netherlands. ²Department of Cell Biology, Radboud Institute for Molecular Life Sciences, The Netherlands. ³Centre for Molecular and Biomolecular Informatics, Radboud Institute for Molecular Life Sciences, The Netherlands. ⁴Translational Metabolic Laboratory, Department Laboratory Medicine, Radboudumc, Nijmegen, The Netherlands. ⁵Department of Pathology, VU University Medical Center, Amsterdam, The Netherlands. ⁶Department of Cell Biology and Histology, Academic Medical Center, Amsterdam, The Netherlands. ⁷Clinical Cooperation Unit Neuropathology, German Cancer Center (DKFZ), Heidelberg, Germany. Correspondence and requests for materials should be addressed to W.P.J.L. (email: william.leenders@radboudumc.nl)

Because of the molecular similarity between α -KG and D-2-HG, the latter can competitively inhibit the activity of a range of α -KG-dependent dioxygenases, of which over 60 have been identified^{9,10}. Most important examples are the Ten-Eleven-Translocation 2 (TET2) DNA demethylases (resulting in the CpG-island hypermethylator phenotype in *IDH^{MUT}* cells) and Jumonji-C (JMJC) histone demethylases (resulting in histone hypermethylation)^{11–13}. The net result is a transcriptional profile that contributes to tumorigenesis via mechanisms that are still poorly understood. Although this has been matter of debate, consensus is now that D-2-HG can promote degradation of the transcription factor hypoxia-inducible factor (HIF-1 α), possibly after non-enzymatic oxidation to α -KG¹⁴. How this exactly contributes to oncogenesis is still an active field of investigation^{15–17}.

The effects of expression of *IDH1*-mutants and/or D-2-HG on tumor metabolism have started to receive attention now¹⁸. It was recently shown that D-2-HG inhibits the tricarboxylic acid (TCA) cycle enzyme succinate dehydrogenase, possibly leading to hypersuccinylation of proteins and anti-apoptotic effects¹⁹. Because mutant *IDH1* lacks isocitrate-to- α -KG conversion activity, normally a predominant source of cytosolic NADPH in the brain²⁰, *IDH^{MUT}* cells are predicted to have lower steady state levels of NADPH, an effect that will be augmented by NADPH-oxidation during D-2-HG production. Thus, *IDH* mutations impact the redox status of glioma cells.

Additionally, *IDH* mutations may affect anabolic pathways: *IDH1/2* can reduce α -KG back to isocitrate which may serve as carbon source for fatty acid and lipid synthesis via citrate and acetyl-CoA^{21,22} but *IDH1^{R132H}* lacks this reverse activity²³. It is conceivable therefore, that *IDH^{MUT}* tumors need metabolic salvage pathways to allow tumor progression and this is supported by the finding of relatively normal α -KG levels in a patient-derived orthotopic *IDH1^{R132H}* oligodendroglioma model²⁴. Because *IDH1^{MUT}* cells display higher sensitivity to glutamine inhibitors than *IDH^{WT}* cells²⁵, glutamine has been proposed to feed into the mitochondrial TCA cycle as an anaplerotic source of α -KG, via the activities of glutaminase and glutamate dehydrogenase (GDH). We previously postulated that gliomas may resort to direct import of glutamate, a ubiquitous neurotransmitter in brain, to allow GDH-mediated α -KG production^{26,27}. NADH/NADPH, generated during this reaction would simultaneously supplement the NAD(P)H pool. These metabolic changes could all play a role in tumor cell maintenance and therefore be an Achilles heel and target for therapeutic inhibition. However, uncoupling the metabolic alterations that result from NADPH/ α -KG depletion from the pleiotropic effects of D-2-HG is a difficult task.

In this study we describe a novel heterozygous *IDH1* mutation which we uncovered by next generation sequencing of a glioblastoma from which a patient-derived xenograft model and corresponding cell line were generated. We show that this *IDH1^{R314C}* mutant does not convert isocitrate to α -KG, unless at non-physiological concentrations of NADP⁺, and does not produce D-2-HG. These properties make that *IDH1^{R314C}* tumor models are valuable tools to study the relevance of α -KG/NADPH depletion versus D-2-HG formation in gliomagenesis and tumor progression.

Results

E98 cells contain a rare heterozygous *IDH1^{R314C}* mutation located in the NADP⁺ binding pocket. The patient-derived E98 astrocytoma model carries a number of glioma-typical genetic mutations and is phenotypically similar to clinical glioma when grown as orthotopic xenografts^{28–30}. This makes this model of high interest as a prototypical glioblastoma model for testing of targeted therapeutics^{31–34}. Because the design of rational targeted therapies requires a detailed analysis of genetic aberrations, we subjected this cell line to targeted genomic next generation sequencing via Ion Torrent analysis using a primer set that allows parallel deep sequencing of 409 genes with known involvement in cancer-related pathways. As we unfortunately did not have access to blood of the E98 donor, SNPs and variants with mean allelic frequency (MAF) > 1% were filtered out using sequence data from pooled blood samples as reference. Due to our general interest in *IDH1*, our attention was specifically drawn to a heterozygous C to T mutation at position 940 in the *IDH1* gene (Fig. 1A) which results in the p.Arg314Cys substitution. Presence of this mutation was verified in the original patient material (Fig. 1B). To check for the incidence of this mutation, 103 DNA samples from glioma (see Supplementary Table 1) were Sanger sequenced. None of these samples contained the p.R314 mutation. Data mining of the Exome Sequencing Project (ESP) database (www.exac.broadinstitute.org/) revealed that this variant has not been identified in 121,410 alleles. Mining of the Cosmic database revealed only one reported *IDH1* c.941G>A/p.R314H mutation in a gastric carcinoma (mutation ID COSM4090677). Thus, the *R314C* mutation is a rare mutation.

Since Arg314 is located in the NADP⁺ binding pocket³⁵ we studied the experimentally solved structure of *IDH1^{WT}* and *IDH1^{R314C}* in complex with NADP⁺ using YASARA. As shown in Fig. 1C, the *R314C* mutation significantly alters the tertiary structure resulting in an imperfect fit of NADP⁺ in the binding pocket, mainly due to the lack of interaction between the negatively charged 2'-phosphate of the co-enzyme NADP⁺ and the positively charged amine group of the arginine, and lack of ionic interactions between the Arg314 and glutamate residues on position 247 and 253 in the other subunit.

***IDH1^{R314C}* is defective in isocitrate to α -KG conversion.** We first examined the activity of purified *IDH1^{R314C}*-GST proteins, using *IDH1^{WT}*-GST and *IDH1^{R132H}*-GST as positive and negative controls. All enzymes could be readily produced and purified (Fig. 2A). Under the conditions tested, both *IDH1^{R132H}*-GST and *IDH1^{R314C}*-GST did not show isocitrate-to- α -KG conversion activity whereas *IDH1^{WT}*-GST did (Fig. 2B). The absence of α -KG formation by *IDH1^{R132H}*-GST and *IDH1^{R314C}* was confirmed with LC-MS (Fig. 2C). Importantly, whereas *IDH1^{R132H}*-GST was active in converting α -KG to D-2-HG (as revealed by oxidation of NADPH) the *IDH1^{R314C}*-GST mutant was completely devoid of this activity (Fig. 2D). Thus, *IDH1^{R314C}* homodimers are inactive in converting isocitrate and NADP⁺ to α -KG and NADPH and, unlike *IDH1^{R132H}*-GST, do not consume NADPH, consistent with the lack of D-2-HG production by E98 xenografts that has already been described before³⁶.

The *IDH1^{R132}* mutation in human gliomas always occurs in a heterozygous manner, resulting in a theoretical 1:2:1 distribution of *IDH^{WT/WT}*, *IDH^{WT/MUT}* and *IDH^{MUT/MUT}* dimers. This stoichiometry may be important for

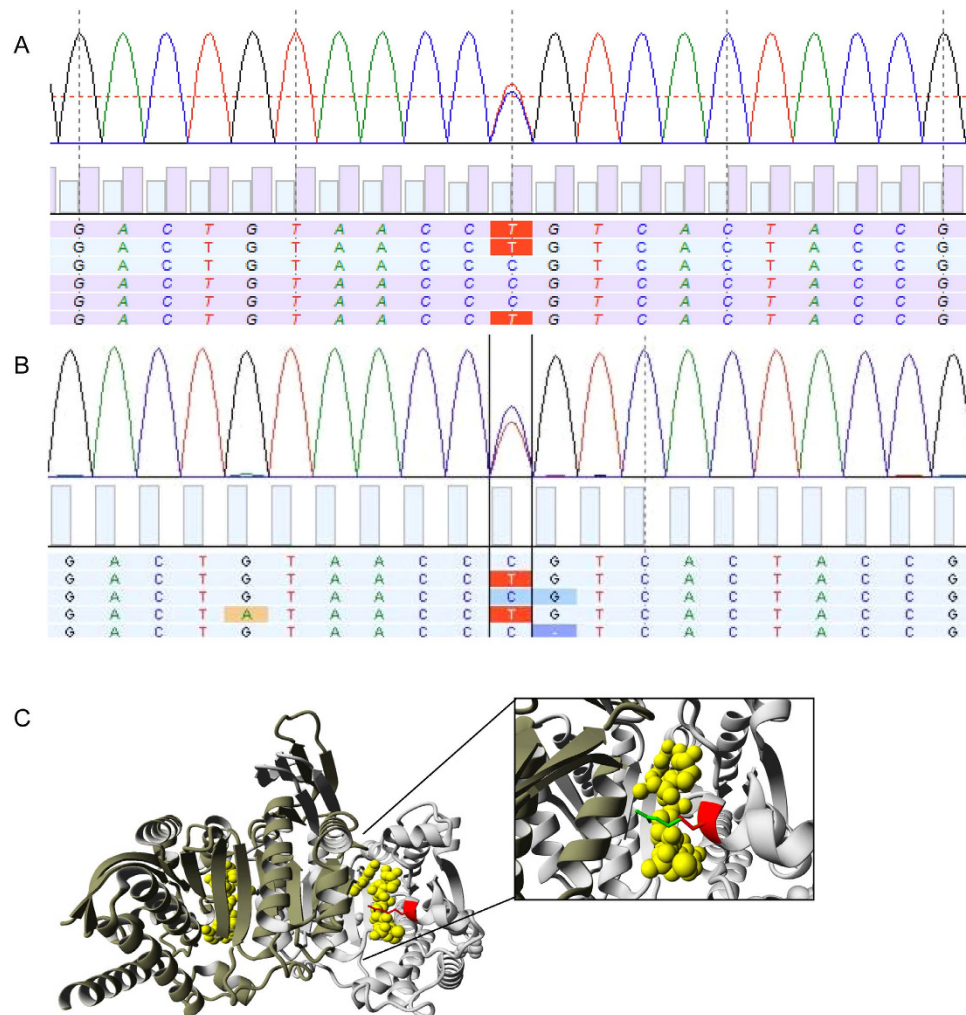


Figure 1. Identification of IDH1^{R314C} in a high grade astrocytoma. (A) Sequencing trace showing the heterozygous C to T mutation at position 940 in the *IDH1* gene found in the E98 cell line and (B) primary tumor material. This mutation leads to the p.Arg314Cys substitution in the IDH1 protein. (C) Display of the 3D- structure of human IDH1^{R314C} generated with YASARA (PDB-file 3innm). The IDH1^{WT} homodimer is displayed with bound cofactor NADP⁺ (yellow), and the arginine residue on position 314 (red), both subunits are coloured in a different shade of grey. The inset shows the mutated cysteine (red) superimposed on the original arginine (green).

balanced IDH activity, because D-2-HG can only be formed via an intimate crosstalk between wild-type and mutant subunits, for which α -KG is a product and substrate, respectively. To analyze the effects of IDH1^{R314C} overexpression in eukaryotic cells we performed enzymatic assays with cell extracts from HEK293T cells, transiently overexpressing IDH1^{WT}, IDH1^{R132H} or IDH1^{R314C} as well as lentivirally transduced LN229 and U251 glioma cells, stably expressing the different IDH1 mutants (Fig. 3A). To be able to distinguish recombinant from endogenous IDH^{WT} and allow statements on IDH^{WT/MUT} ratios we equipped the mutated reading frames with a BAPHIS (biotin-acceptor peptide-8xHis) tag, increasing molecular weight with ~3 kDa. Intriguingly, irrespective of the method of genetic modification (transfection or lentiviral transduction) expression levels of recombinant enzymes were lower than that of the endogenous enzymes, with IDH^{R132H} consistently being lowest, possibly a result of negative selection for IDH1^{R132H}-BAPHIS overexpression and associated toxic levels of D-2-HG³⁷. Consistent with the absence of activity of purified IDH1^{R314C} homodimers (Fig. 2B), for all cell lines NADP⁺-dependent oxidative decarboxylation of isocitrate was significantly lower in IDH1^{R314C}-BAPHIS expressing cells than in IDH1^{WT}-BAPHIS cells (Fig. 3B). Of note, the reduced activity of IDH1^{R314C}-BAPHIS in U251 cell extracts could be rescued by performing the enzymatic assay in supraphysiological concentrations of NADP⁺ (Supplementary Figure 1), in line with loss of NADP⁺-affinity as predicted from the solved structure in Yasara, and as described earlier by Lee *et al.*³⁵. Consistent with this model, the R314C mutation caused an eight-fold increase in Km for NADP⁺ (318 μ M vs 38 μ M for IDH^{WT}, Fig. 3C). This predicts that IDH1^{R314C} is inactive under physiological NADP⁺ concentrations. Of note, activity of GST-IDH1^{R314C} homodimers at higher concentrations of NADP⁺ was too low to calculate Km for isocitrate.

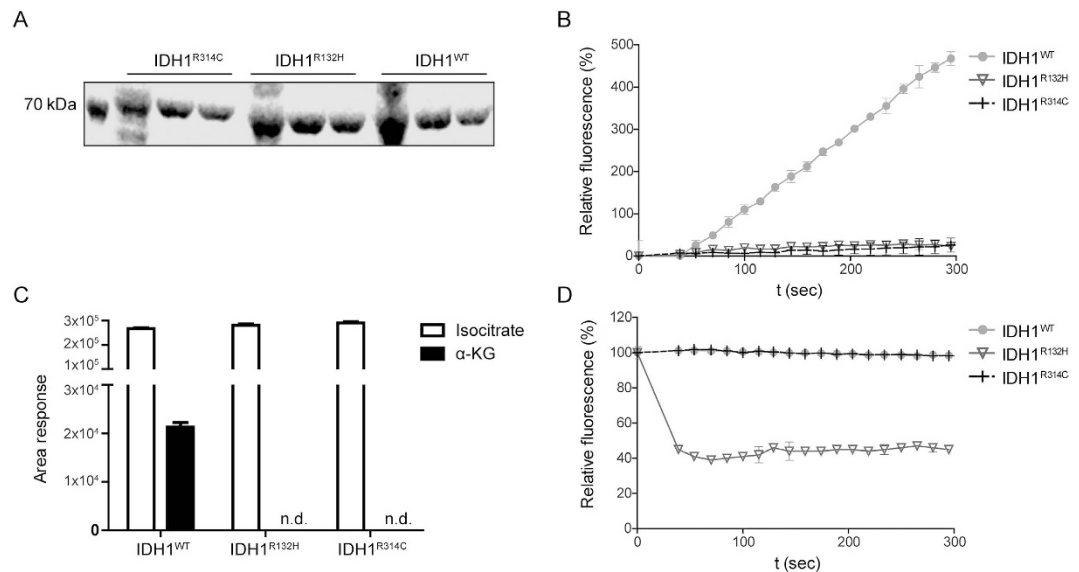


Figure 2. Homodimeric IDH1^{R314C}-GST is defective in the isocitrate-to α -KG reaction and does not produce D-2-HG. (A) SDS-page gel stained with coomassie brilliant blue showing expression of purified IDH1-GST constructs. (B) Fluorescent monitoring of NADPH formation at 340 nm shows that only purified IDH1^{WT}-GST is capable to convert isocitrate to α -KG under the reaction conditions tested, whereas IDH1^{R132H}-GST and IDH1^{R314C}-GST are inactive. (C) α -KG production by IDH1-GST enzymes was measured with LC-MS. Note that only IDH1^{WT}-GST is capable of isocitrate-to- α -KG conversion. (n.d. = non detectable, area < 150). (D) Fluorescent monitoring of NADPH reduction shows that only purified IDH1^{R132H}-GST is active in the α -KG-to-D-2-HG conversion. Both IDH1^{WT}-GST and IDH1^{R314C}-GST lack the capability to produce D-2-HG.

As expected from the lack of NADPH consumption when incubated with α -KG (Fig. 2D), IDH1^{R314C}-BAPHIS expressing LN229 and U251 glioblastoma cell lines did not produce 2-HG, in contrast to their IDH1^{R132H}-BAPHIS counterparts (Fig. 3D).

Discussion

Since their discovery, hotspot mutations in IDH enzymes have become a major focus of research. The oncogenic potential of IDH1^{R132H} has been attributed to epigenetic alterations, resulting from the production of the alleged oncometabolite D-2-HG^{9,10,38}. Furthermore it has been shown that proliferation of IDH1^{R132H} cells requires metabolic rescue programs that depend on *in vivo* tumor-stroma interactions, possibly involving glutamate import²⁶.

We here identify and characterize IDH1^{R314C}, a novel and rare mutation in IDH1 in a high grade astrocytoma which has not been reported before. We show that IDH1^{R314C} has a greatly reduced affinity for NADP⁺, in agreement with a previous structure-function relationship study on porcine IDH1³⁵ and is consequently defective in oxidizing isocitrate to α -KG. The R314C mutation did not shift the cofactor dependency from NADP⁺ to NAD⁺ (Supplementary Figure 2) as was previously reported for mutated IDH1 from the halobacterium *Haloferrax Volcanii*³⁹.

To define an exact role for IDH1^{R314C} in tumor formation and biological behavior of cancer cells is impossible in the context of the many more mutations that are found in E98⁴⁰. To study this further, isogenic E98 cell lines with a repaired IDH1^{R314R} allele are required and such technically challenging cell lines are not yet available.

The decreased potential of IDH1^{R314C} cells to produce α -KG and NADPH in the cytosol may directly impact on redox potential, lipid synthesis and membrane production and may explain the slow growth rates of E98 cells *in vitro* (doubling time of 46 hrs, data not shown). Interestingly, despite these very slow growth rates, *in vivo* E98 xenografts represent the most aggressive diffuse infiltrative brain tumor model in our lab, killing mice within 4–5 weeks after intracerebral implantation²⁸. This illustrates that the brain micro-environment is crucially involved in allowing growth of E98 cells. Since the redox status of cells may particularly impact on cell migration⁴¹ it would be of high interest to investigate how relatively low NADPH/NADP⁺ ratios in E98 cells *in vivo* are associated with active cell migration, leading to the diffuse infiltrative phenotype. Further unraveling of the specific *in vivo* metabolic salvage pathways that are adapted by E98 cells and may be involved in its aggressive behavior may lead to potential novel ways for therapeutic intervention.

In oncology, most NGS protocols aim for detection of actionable hot spot mutations in known genes only, leaving a potentially huge amount of mutations with significance for tumor biology, undetected and this is the reason why we only now recognized that E98 cells carry the IDH1^{R314C} mutation²⁴. Alterations in genes encoding metabolic enzymes may be directly or indirectly involved in tumorigenesis based on subtle distortions in equilibria between metabolic intermediates and/or oxidative milieu.

In conclusion, we identified a novel IDH1^{R314C} mutant that shares with the common IDH1^{R132H} mutant a defect in isocitrate-to- α -KG conversion activity, but lacks the capacity to produce D-2-HG. Future comparative

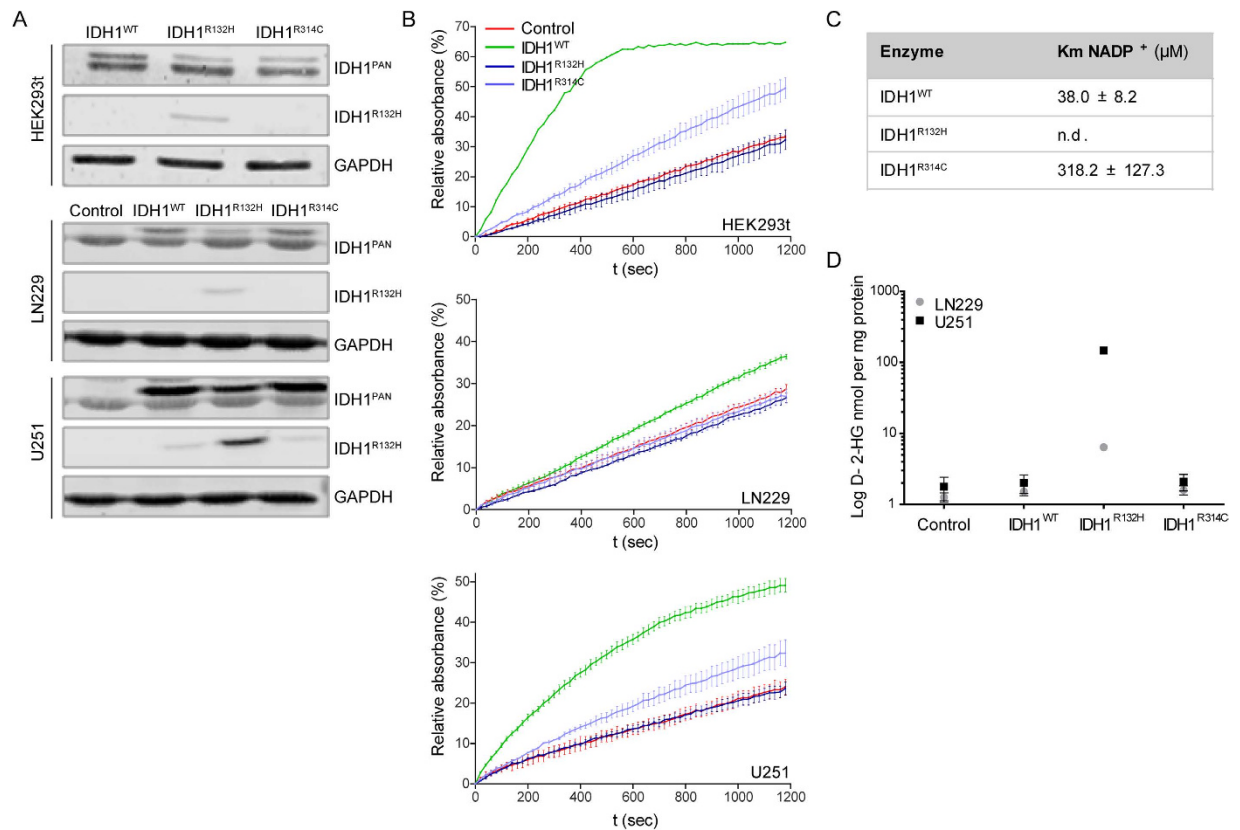


Figure 3. IDH1^{R314C}-BAPHIS expression in glioma cell lines leads to reduced forward activity compared to IDH1^{WT} expression. (A) Western blots showing expression of IDH1-BAPHIS in transiently transfected HEK293t and lentivirally transduced LN229 and U251 glioma cells. Blots were stained with anti-IDH1^{PAN} and anti-IDH1^{R132H} as indicated, or with anti-GAPDH as a loading control. Since the recombinant proteins are ~3 kDa larger than endogenous IDH1 they can be distinguished from the endogenous IDH1. Control LN229 and U251 were transduced with empty vector virus (EV). (B) Monitoring of NADPH formation after isocitrate/NADP⁺ addition to extracts from transfected/transduced cell lines. NADPH formation was monitored by absorbance measurements at 340 nm. Note that IDH1^{R314C}-BAPHIS was far less effective in oxidative carboxylation of isocitrate than IDH1^{WT}-BAPHIS. (C) Km values of IDH1-GST for NADP⁺. The Km value for NADP⁺ for IDH1^{R132H}-GST could not be determined. (D) D-2-HG production by IDH1-BAPHIS expressing cell lines was measured with LC-MS. Only IDH1^{R132H}-BAPHIS expressing cells were capable of D-2-HG production.

profiling studies using isogenic cell lines expressing IDH1^{WT}, IDH1^{R132H} or IDH1^{R314C} will allow us to distinguish between epigenetic and metabolic alterations, resulting from NADPH/ α -KG depletion or D-2-HG accumulation.

Methods

E98. Generation of the E98 model which was derived from a grade IV astrocytoma, was described before²⁸. All animal experimental work was performed in accordance with the guidelines of and was approved by the local ethical committee for animal experimentation of Radboud University. An adherent E98 cell line was generated from mouse xenografts via routine procedures^{29,40} and cultured in DMEM (Lonza, Basel, Switzerland) supplemented with 10% FCS (Gibco, ThermoFisher Scientific, Waltham, MA, USA) and 40 μg/ml gentamycin (Centrafarm, Etten-Leur The Netherlands).

Next generation sequencing. Genomic DNA from E98 cells and from original tumor material was analyzed by semi-conductor sequencing (IonPGM, Life Technologies, ThermoFisher Scientific, Waltham, MA, USA) using the comprehensive cancer panel (Life Technologies, ThermoFisher Scientific, Waltham, MA, USA) detecting copy number variations and mutations in 409 cancer-related genes. An IonPGM E98 library was generated according to the manufacturer's protocol. In short, 10 ng of DNA per pool was amplified in 21 cycles by PCR using the Ion AmpliSeqTM mastermix, followed by barcode and adapter ligation. Amplified products were purified with Agencourt AMPure XP beads (Beckman Coulter Genomics, High Wycombe, UK). The library was diluted to 20 pM and emulsion PCR was performed using the Ion OneTouchTM 200 Template kit following the manufacturer's protocol. Next, Ion Sphere Particles (ISPs) were recovered and enriched for template positive ISPs using Dynabeads MyOne Streptavidin C1 beads (Life Technologies, ThermoFisher Scientific, Waltham, MA, USA) in the Ion OneTouchTM ES instrument (Life Technologies, ThermoFisher Scientific, Waltham, MA, USA). ISP enrichment was quantified using the Qubit 2.0 fluorometer (Life Technologies, ThermoFisher Scientific, MA,

USA). Sequencing primer and polymerase were added to the final enriched spheres before loading onto an Ion 318 chip according to the Ion PGMTM 200 sequencing kit protocol. Variants were called using NextGene (JSI) and filtered for common variants (MAF > 1%) in the general population.

Visualization of IDH1 structure with YASARA. The structure of human IDH1 has been experimentally solved and can be found in PDB-file 3inm⁸. We used the WHAT IF & YASARA twinset for visualization and analysis^{42,43}.

PCR and cloning of IDH1 constructs. Total RNA was isolated from cell lines using TRIzol reagent (Life Technologies, ThermoFisher Scientific, Waltham, MA, USA) and converted to cDNA using oligo-dT and MMLV reverse transcriptase (New England Biolabs, Ipswich, MA, USA) using standard protocols. Open reading frames for *IDH1*^{WT}, *IDH1*^{R132H} and *IDH1*^{R314C} were PCR amplified from HT29, E478 and E98 cDNA, respectively, using primers IDH-EcoRIFw [5'-CGAATTCAGTGTCAAGGTTTATTGAAGTC-3'] and IDH-AgeIRev [5'-CACCGGTAAGTTTGGCCTGAGCTAG-3'] and Phusion DNA polymerase (Finnzymes, ThermoFisher Scientific, Waltham, MA, USA). PCR products were digested with EcoRI and AgeI (New England Biolabs, Ipswich, MA, USA) and cloned in fusion to a C-terminal biotin-acceptor peptide (BAP) and an 8xhis tag (HIS) in vector PHLsec-BAPHIS AgeI/EcoRI, derived from PHLsec-HIS (Addgene, Cambridge, MA, USA) using T4 DNA ligase (New England Biolabs, Ipswich, MA, USA). The BAPHIS tags were added to distinguish recombinant from endogenous IDH by molecular weight and to allow Ni-bead purification. Clones containing the respective mutations were selected via Sanger sequencing. For generation of lentiviral constructs, the different ORFs were recloned in vector pENTRY which was recombined with pLENTI using the GATEWAY system via standard procedures.

In parallel, IDH ORFs were cloned in fusion with GST in *E. coli* expression vector pDEST15 as described before³⁷.

GST fusion protein expression and purification. GST fusion proteins were expressed in *E. coli* strain ER2566 via standard induction protocols. Briefly, 2xTY medium supplemented with 50 µg/ml ampicillin (Roche, Basel, Switzerland) was inoculated with 1% v/v overnight culture. Protein expression was induced with 1 mM IPTG (Serva, Heidelberg, Germany) at OD₆₀₀~0.6. After 3 hours at 30 °C, bacteria were harvested by centrifugation and resuspended in 300 mM NaCl, 50 mM TRIS/HCL pH 8.0 supplemented with Complete protease inhibitor (Roche, Basel, Switzerland). Cells were lysed by 3 freeze-thaw cycles, followed by sonication (4 × 15 seconds, 25% amplitude, Bioruptor, Diagenode) and centrifugation (3500 rpm, 20 min). Proteins were purified using glutathione beads (Pierce, ThermoFisher Scientific, Waltham, MA, USA), eluted with 10 mM glutathione and dialyzed extensively against 150 mM NaCl, 25 mM TRIS/HCL pH 7.5. Expression and purity were checked by SDS-PAGE gel electrophoresis and Coomassie Brilliant Blue staining.

Transient transfection experiments. HEK293T cells were grown to 30% confluence in 6 wells plates in DMEM supplemented with 10% FCS and 40 µg/ml gentamycin. Cells were transfected with 2 µg pHLsec-IDH1^{MUT}-BAPHIS, IDH1^{WT}-BAPHIS or pIRESneo-EGFP using Fugene HD reagent according to the manufacturers' protocol (Roche, Basel, Switzerland). After 2 days, cells were harvested and processed to cell lysates by scraping in 150 µl sucrose buffer (0.32 M sucrose in 10 mM TRIS-HCL pH 7.5) and sonicating on ice (3 cycles of 30 sec max power and 30 sec off in Bioruptor, Diagenode). Lysates were centrifuged (14000 rpm, 10 min, 4 °C) and supernatants were subjected to BCA assays (Pierce, ThermoFisher Scientific, Waltham, MA, USA) for protein concentration measurements and stored at -20 °C until further analysis. To quantify IDH1 protein expression, 20 µg of total cytosolic protein was subjected to 10% SDS-PAGE and electroblotted onto a nitrocellulose membrane (Whatman Optitran BA-S85, GE healthcare, Little Chalfont, UK). After blocking in Odyssey Blocking buffer (LI-COR biosciences, Lincoln, NE, USA) in PBS (1:1) the membrane was incubated with rabbit-anti-IDH1 (1:1000, HPA035248, Sigma-Aldrich, St. Louis, MO, USA) and mouse-anti-IDH1R132H (1:400, H09L, Dianova, Hamburg, Germany) in blocking buffer, followed by incubation with goat-anti-mouseDyLight800 (1:10.000, ThermoFisher Scientific, Waltham, MA USA) or goat-anti-rabbitAlexa680 (1:10.000, Invitrogen, ThermoFisher Scientific, Waltham, MA, USA). After washing, blots were analyzed on the Odyssey scanner (LI-COR biotechnology, Lincoln, NE, USA).

Generation of stable IDH1^{MUT} overexpression glioma cell lines. LN229 and U251 cells were transduced with lentiviral vectors encoding IDH1^{WT}-BAPHIS, IDH1^{R132H}-BAPHIS, IDH1^{R314C}-BAPHIS or an empty vector (EV) control as described before⁴⁴. Transduced cells were selected using blasticidin and cultured in DMEM supplemented with 10% FCS and 40 µg/ml gentamycin. Cells were grown to 80% confluency in 10 cm ø culture plates (Corning, Corning, NY, USA). Cell culture media were collected and stored at -20 °C until later analysis. Cells were collected and cytosolic extracts were prepared in 400 µl sucrosebuffer as described before. Twenty µg of protein was subjected to SDS-PAGE gel electrophoresis and western blot to quantify protein expression.

IDH activity measurements. Isocitrate-to-α-KG and α-KG-to-2-HG conversion rates of the purified IDH1-GST enzymes were determined by monitoring NADPH generation over time. Assays were performed in 100 µl freshly prepared assay solution (2 mM MgCl₂ in 100 mM TRIS/HCL pH 7.4) containing 10 mM NADP⁺ (Sigma-Aldrich, St. Louis, MO, USA) and 10 mM isocitrate (Sigma-Aldrich, St. Louis, MO, USA) (forward assay) or 10 mM NADPH (Sigma-Aldrich, St. Louis, MO, USA) and 10 mM α-KG (Sigma-Aldrich, St. Louis, MO, USA) (reverse assay). Four µg of purified IDH1-GST fusion proteins were incubated with assay solution in a 96 wells plate at 37 °C (BD Falcon, Franklin Lakes, USA) and fluorescence (Ex. 340 +/- 10 nm, Em. 440 +/- 10 nm), was measured every 15 seconds over a period of 5 minutes with an Omega FluoStar (BMG Labtech, Ortenberg, Germany). To examine enzyme kinetics in more detail, 4 µg of IDH1-GST proteins were incubated with varying

MRM	Compound name	cone V (V)	Coll eV (eV)	Ret. time (min)
191 > 111	Isocitrate	22	13	1.28
145 > 101	α -KG	22	8	1.53
147 > 129	D-2-HG	19	11	1.54
152 > 134	$^{13}\text{C}_5$ -2-HG	19	11	1.54

Table 1. MRM transitions for metabolite detection. note: $t_0 = 0.8$ min.

NADP⁺ concentrations (0–500 μM) and 100 μM isocitrate at 22 °C. Absorbance at 340 nm was measured every 20 seconds with a Benchmark Plus Microplate Spectrophotometer (Bio-Rad, Hercules, CA, USA). Non-linear regression analysis (Michaelis-Menten) was performed in Graphpad Prism 5.03.

To determine NAD⁺ dependency, 4 μg of IDH1-GST proteins were incubated with 100 μl assay solution containing 2 mM MgCl₂, 500 μM isocitrate and 2, 5 mM NAD⁺ (Sigma-Aldrich, St. Louis, MO, USA) in 100 mM TRIS-HCL pH 7.4 at 22 °C. A sucrose extract made from human liver was taken as a control. Absorbance at 340 nm was monitored as described.

For enzyme measurements in extracts of eukaryotic cells, 50 μg of total cytosolic protein were incubated with assay solution (2 mM MgCl₂, 500 μM isocitrate in 100 mM TRIS/HCL pH 7.4) containing 100 μM NADP⁺ in 96 wells plates (Greiner) at 22 °C and NADPH generation was quantified as described before.

D-2-HG, α -KG and isocitrate measurements by isotope dilution LC-MS. D-2-HG levels in cell culture media were measured using stable isotope dilution liquid chromatography tandem mass spectrometry (LC-MS) as described before³⁶.

α -KG and isocitrate levels were determined in *in vitro* IDH1 reaction mixtures. 4 μg of IDH1-GST proteins were incubated in 150 μl freshly prepared assay solution (2 mM MgCl₂ in 100 mM TRIS/HCL pH 7.4) containing 500 μM isocitrate and 100 μM NADP⁺. After 20 min incubation at 22 °C the reaction was stopped using 20 μl 4% HCOOH. 25 μl of this solution was mixed with 25 μl 9 μM $^{13}\text{C}_5$ -2-HG stable isotope (Chiralex, Nijmegen, The Netherlands) in deionized water and 75 μl deionized water before passing it through an Amicon Ultra 30 kDa Centrifugal Filter (Merck Millipore, Billerica, MA, USA) by centrifugation (14000 g, 30 min). 2 μl of the filtrate was injected onto a Atlantis T3 HPLC Column (2.1*100 mM dp 3 μm) and run with 12.5% MeOH in 87.5% 0.3% HCOOH in water. The column was connected to a Waters Quattro Premier tandem mass spectrometry fitted with an ESI probe operated in negative mode, recording the following MRM transitions, as summarized in Table 1.

Statistics. All experiments were performed in triplicate. Data were processed in Excell (Microsoft, Redmond, WA, USA) and enzyme kinetics were determined by fitting of Michaelis Menten in Graphpad Prism 5.03 (Graphpad Software, La Jolla, CA, USA).

References

- Sahm, F. *et al.* Farewell to oligoastrocytoma: *in situ* molecular genetics favor classification as either oligodendroglioma or astrocytoma. *Acta Neuropathol* **128**, 551–559 (2014).
- Louis, D. N., Ohgaki, H., Wiestler, O. D. & Cavenee, W. K. Classification of Tumours of the Central Nervous System. *WHO* (2007).
- Stupp, R. *et al.* Radiotherapy plus concomitant and adjuvant temozolomide for glioblastoma. *N Engl J Med* **352**, 987–996 (2005).
- Parsons, D. W. *et al.* An integrated genomic analysis of human glioblastoma multiforme. *Science* **321**, 1807–1812 (2008).
- Bals, J. *et al.* Analysis of the IDH1 codon 132 mutation in brain tumors. *Acta Neuropathol* **116**, 597–602 (2008).
- Bleeker, F. E. *et al.* IDH1 mutations at residue p.R132 (IDH1(R132)) occur frequently in high-grade gliomas but not in other solid tumors. *Hum Mutat* **30**, 7–11 (2009).
- Hartmann, C. *et al.* Type and frequency of IDH1 and IDH2 mutations are related to astrocytic and oligodendroglial differentiation and age: a study of 1,010 diffuse gliomas. *Acta Neuropathol* **118**, 469–474 (2009).
- Dang, L. *et al.* Cancer-associated IDH1 mutations produce 2-hydroxyglutarate. *Nature* **462**, 739–744 (2009).
- Xu, W. *et al.* Oncometabolite 2-hydroxyglutarate is a competitive inhibitor of alpha-ketoglutarate-dependent dioxygenases. *Cancer Cell* **19**, 17–30 (2011).
- Borodovsky, A., Seltzer, M. J. & Riggins, G. J. Altered cancer cell metabolism in gliomas with mutant IDH1 or IDH2. *Curr Opin Oncol* **24**, 83–89 (2012).
- Lu, C. *et al.* IDH mutation impairs histone demethylation and results in a block to cell differentiation. *Nature* **483**, 474–478 (2012).
- Chowdhury, R. *et al.* The oncometabolite 2-hydroxyglutarate inhibits histone lysine demethylases. *EMBO Rep* **12**, 463–469 (2011).
- Xu, W. *et al.* Oncometabolite 2-hydroxyglutarate is a competitive inhibitor of alpha-ketoglutarate-dependent dioxygenases. *Cancer Cell* **19**, 17–30 (2011).
- Tarhonskaya, H. *et al.* Non-enzymatic chemistry enables 2-hydroxyglutarate-mediated activation of 2-oxoglutarate oxygenases. *Nat Commun* **5**, 3423 (2014).
- Koivunen, P. *et al.* Transformation by the (R)-enantiomer of 2-hydroxyglutarate linked to EGLN activation. *Nature* **483**, 484–488 (2012).
- Blouw, B. *et al.* The hypoxic response of tumors is dependent on their microenvironment. *Cancer Cell* **4**, 133–146 (2003).
- Molenaar, R. J., Radivoyevitch, T., Maciejewski, J. P., van Noorden, C. J. & Bleeker, F. E. The driver and passenger effects of isocitrate dehydrogenase 1 and 2 mutations in oncogenesis and survival prolongation. *Biochimica et biophysica acta* (2014).
- Parker, S. J. & Metallo, C. M. Metabolic consequences of oncogenic IDH mutations. *Pharmacology & therapeutics* **152**, 54–62 (2015).
- Li, F. *et al.* NADP-IDH Mutations Promote Hypersuccinylation that Impairs Mitochondria Respiration and Induces Apoptosis Resistance. *Mol Cell* **60**, 661–675 (2015).
- Bleeker, F. E. *et al.* The prognostic IDH1(R132) mutation is associated with reduced NADP+-dependent IDH activity in glioblastoma. *Acta Neuropathol* **119**, 487–494 (2010).
- Wise, D. R. *et al.* Hypoxia promotes isocitrate dehydrogenase-dependent carboxylation of alpha-ketoglutarate to citrate to support cell growth and viability. *Proc Natl Acad Sci USA* **108**, 19611–19616 (2011).
- Metallo, C. M. *et al.* Reductive glutamine metabolism by IDH1 mediates lipogenesis under hypoxia. *Nature* **481**, 380–384 (2012).

23. Leonardi, R., Subramanian, C., Jackowski, S. & Rock, C. O. Cancer-associated isocitrate dehydrogenase mutations inactivate NADPH-dependent reductive carboxylation. *J Biol Chem* **287**, 14615–14620 (2012).
24. Navis, A. C. *et al.* Increased mitochondrial activity in a novel IDH1-R132H mutant human oligodendroglioma xenograft model: *in situ* detection of 2-HG and alpha-KG. *Acta Neuropathol Commun* **1**, 18 (2013).
25. Seltzer, M. J. *et al.* Inhibition of glutaminase preferentially slows growth of glioma cells with mutant IDH1. *Cancer Res* **70**, 8981–8987 (2010).
26. van Lith, S. A. *et al.* Glutamate as chemotactic fuel for diffuse glioma cells: are they glutamate suckers? *Biochimica et biophysica acta* **1846**, 66–74 (2014).
27. van Lith, S. A., Molenaar, R., van Noorden, C. J. & Leenders, W. P. Tumor cells in search for glutamate: an alternative explanation for increased invasiveness of IDH1 mutant gliomas. *Neuro Oncol* (2014).
28. Claes, A. *et al.* Phenotypic and genotypic characterization of orthotopic human glioma models and its relevance for the study of anti-glioma therapy. *Brain Pathol* **18**, 423–433 (2008).
29. Navis, A. C. *et al.* Effects of dual targeting of tumor cells and stroma in human glioblastoma xenografts with a tyrosine kinase inhibitor against c-MET and VEGFR2. *PLoS One* **8**, e58262 (2013).
30. Navis, A. C. *et al.* Identification of a novel MET mutation in high-grade glioma resulting in an auto-active intracellular protein. *Acta Neuropathol* **130**, 131–144 (2015).
31. Claes, A. & Leenders, W. Vessel normalization by VEGF inhibition. *Cancer Biol Ther* **7**, 7 (2008).
32. Claes, A. *et al.* Antiangiogenic compounds interfere with chemotherapy of brain tumors due to vessel normalization. *Mol Cancer Ther* **7**, 71–78 (2008).
33. Navis, A. C. *et al.* Effects of targeting the VEGF and PDGF pathways in diffuse orthotopic glioma models. *J Pathol* **223**, 626–634 (2011).
34. Hamans, B. *et al.* Multivoxel 1H MR spectroscopy is superior to contrast-enhanced MRI for response assessment after antiangiogenic treatment of orthotopic human glioma xenografts and provides handles for metabolic targeting. *Neuro Oncol* **15**, 1615–1624 (2013).
35. Lee, P. & Colman, R. F. Implication by site-directed mutagenesis of Arg314 and Tyr316 in the coenzyme site of pig mitochondrial NADP-dependent isocitrate dehydrogenase. *Archives of biochemistry and biophysics* **401**, 81–90 (2002).
36. Navis, A. C. *et al.* Increased mitochondrial activity in a novel IDH1-R132H mutant human oligodendroglioma xenograft model: *in situ* detection of 2-HG and α -KG. *Acta Neuropathol Commun* **1**, 18 (2013).
37. Pusch, S. *et al.* D-2-Hydroxyglutarate producing neo-enzymatic activity inversely correlates with frequency of the type of isocitrate dehydrogenase 1 mutations found in glioma. *Acta Neuropathol Commun* **2**, 19 (2014).
38. Loenarz, C. & Schofield, C. J. Expanding chemical biology of 2-oxoglutarate oxygenases. *Nature chemical biology* **4**, 152–156 (2008).
39. Rodriguez-Arnedo, A., Camacho, M., Llorca, F. & Bonete, M. J. Complete reversal of coenzyme specificity of isocitrate dehydrogenase from *Haloferax volcanii*. *The protein journal* **24**, 259–266 (2005).
40. Navis, A. C. *et al.* Identification of a novel MET mutation in high-grade glioma resulting in an auto-active intracellular protein. *Acta Neuropathol* (2015).
41. van Horssen, R. *et al.* Intracellular NAD(H) levels control motility and invasion of glioma cells. *Cell Mol Life Sci* **70**, 2175–2190 (2013).
42. Krieger, E., Koraimann, G. & Vriend, G. Increasing the precision of comparative models with YASARA NOVA—a self-parameterizing force field. *Proteins* **47**, 393–402 (2002).
43. Vriend, G. WHAT IF: a molecular modeling and drug design program. *Journal of molecular graphics* **8**, 52–56, 29 (1990).
44. Esmaeili, M. *et al.* IDH1 R132H mutation generates a distinct phospholipid metabolite profile in glioma. *Cancer Res* **74**, 4898–4907 (2014).

Acknowledgements

SvL is supported by a Radboudumc grant, KL is supported by a grant of the Dutch Cancer Society (grant UVA 2014-6839), ACN is supported by the STOPbraintumors Foundation (Stichting STOPhersentumoren.nl).

Author Contributions

S.A.M.v.L., A.C.N. and W.P.J.L. wrote the manuscript and prepared the figures, W.P.J.L., S.A.M.v.L. and K.V. produced recombinant proteins, K.L., K.V. and S.P. performed biochemical assays, N.S. and B.T. performed NGS and validated mutations, J.T.G.S. and W.J.A.J. performed molecular cloning, S.A.M.v.L. and H.V. analyzed the YASARA model, R.A.W. and A.v.R. performed LC-MS, W.P.J.L., S.A.M.v.L., P.W., R.J.M. and C.J.F.v.N. were involved in the conceptual design of experiments and manuscript. All authors reviewed the manuscript.

Additional Information

Supplementary information accompanies this paper at <http://www.nature.com/srep>

Competing financial interests: The authors declare no competing financial interests.

How to cite this article: van Lith, S. A. M. *et al.* Identification of a novel inactivating mutation in Isocitrate Dehydrogenase 1 (IDH1-R314C) in a high grade astrocytoma. *Sci. Rep.* **6**, 30486; doi: 10.1038/srep30486 (2016).



This work is licensed under a Creative Commons Attribution 4.0 International License. The images or other third party material in this article are included in the article's Creative Commons license, unless indicated otherwise in the credit line; if the material is not included under the Creative Commons license, users will need to obtain permission from the license holder to reproduce the material. To view a copy of this license, visit <http://creativecommons.org/licenses/by/4.0/>

© The Author(s) 2016